ELSEVIER

Polymer 42 (2001) 217–226

polymer

www.elsevier.nl/locate/polymer

Electron paramagnetic resonance of poly(benzazole)s and conducting properties of N^+-implanted poly(benzazole)s

Shanfeng Wang, Pingping Wu*, Zhewen Han

Department of Polymer Science and Engineering, East China University of Science and Technology, Shanghai 200237, People's Republic of China

Received 8 December 1999; received in revised form 1 March 2000; accepted 14 April 2000

Abstract

We present electron paramagnetic resonance (EPR) studies of the magnetic defect in poly(benzazole)s (including poly(*p*-phenylene benzobisthiazole) (PBZT), poly(*p*-phenylene benzobisoxazole) (PBO), poly(2,5-benzoxazole) (ABPBO), PBO–ABPBO and poly(1,4-phenylene benzobisoxazole-*co*-dimethylene benzobisoxazole) (PBO–PBOC2)) and the model compounds. Temperature dependence of the EPR spectra of poly(benzazole)s over the range 100–300 K and the effect of heat-treatment temperature on EPR parameters were also discussed. $FeCl_3 \cdot 6H_2O$-doped PBZT was investigated in its EPR signals. The results of analyses of the detailed lineshapes and linewidths were discussed in terms of the soliton–antisoliton, polaron and bipolaron model of the magnetic defect. After that, the conductivity studies and Raman characterization of N^+-implanted PBZT and PBO were reported. The room-temperature conductivity of these implanted polymers, approximately 0.1–10 S cm^{-1}, is significantly higher than that of pristine polymers. It was revealed through Raman spectrum that the conductivity was attributed partially to the graphite laminar formed in the process of ion-implantation. The results of these studies contribute toward an identification of the origin and nature of the paramagnetic centers in poly(benzazole)s and toward an understanding of the charge transport mechanism.

Keywords: Electron paramagnetic resonance; Poly(benzazole)s; Ion-implantation

1. Introduction

A number of conducting polymers with π-conjugated system have been studied in the 1980s because of their promising application in various areas of technology [1–3]. Interest in magnetic properties of the *trans*-$(CH)_x$ and doped *trans*-$(CH)_x$ attracted considerable attention from the scientific community, ranging from chemistry to particle physics and field theory, as well as condensed matter physics [4–7]. The studies of polyacetylene have stimulated an awareness of the potential importance of the generation of new concepts, which are of great interest to physics and chemistry. Unfortunately, these conjugated polymers, including polyacetylene and poly(*p*-phenylene), suffered from environmental instability, intractability and degradation upon doping in various degrees.

Aromatic heterocyclic polymers of the poly(benzazole) family were studied since the early 1980s [8,9]. As illustrated in Fig. 1, the rigid-rod or semi-rigid structures of these kinds of polymer bring about many outstanding mechanical properties and thermal stability. These heterocyclic aromatic conjugated polymers belong to a class of rigid chain polymers rather than polyacetylene-type coil polymers. Because of the co-linear co-planar and aromatic structure, which suggests a possible pathway for delocalization and charge transport, this class of polymers is believed to be highly conjugated and is favorably considered to be a base material for conducting polymers.

Mark et al. [10,11] calculated electronic band structures for the poly(*p*-phenylene benzobisoxazole) (PBO), poly(*p*-phenylene benzobisthiazole) (PBZT) and poly(2,5-benzoxazole) (ABPBO) chains by quantum-mechanical methods. For *cis*-PBO and *trans*-PBT chains in their coplanar conformations, the band gaps in the axial direction were found to be 1.72 and 1.73 eV, respectively. And at a rotation angle $\phi = 23°$, about the C–C bond joining the two ring systems in the repeat unit for PBZT, the value of the band gap is 1.98 eV. The similar case for ABPBO is 2.31 eV. The values are close to the corresponding experimental values 1.4–1.8 eV reported for *trans*-polyacetylene, which should suggest promise of being semiconducting polymers.

Yet, investigations on the conducting and paramagnetic properties of these polymers were very few. It was believed that chemical or electrochemical methods of doping were not possible due to lack of a suitable solvent [12], or due to a

* Corresponding author. Tel.: +8621-64253060; fax: +8621-64233269.
E-mail address: zhwhan@ecust.edu.cn (P. Wu).

0032-3861/01/$ - see front matter
PII: S0032-3861(00)00315-3

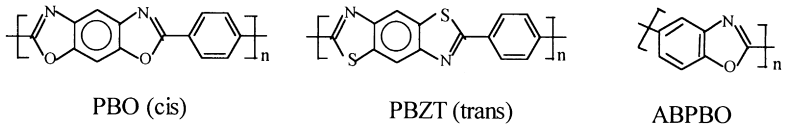

Fig. 1. Chemical structures of the poly(benzazole)s discussed herein.

close packed lattice that prevents intercalation [13]; moreover, somewhat high ionization potential is expected from amide groups in the polymers [14]. In fact, the experimental results indicated that the doped conductivity of these polymers was not high [14]. Jenekhe et al. [15] and Wang et al. [16] reported on the studies of $^{84}Kr^{+}$-implanted conducting rigid-rod polymers and other ladder polymers. This method could obtain satisfying results ($\sim$50–240 S cm^{-1}).

It was reported [17] that poly(benzazole)s had significant electron paramagnetic resonance (EPR) signals. But unfortunately in the report cited above, the EPR signals were thought as the result of radicals generated by scission of C–C bonds along the polymer chains, which was apparently wrong. Dalton et al. [18] gave the proper explanation. However, much less detailed EPR research has been done on these polymers. Nevertheless, such research can yield interesting information about the origin and nature of the electrons, which will contribute to the observed electrical conductivity and paramagnetic properties.

2. Experimental

The PBZ samples were prepared in our own laboratory according to previous reports [19–21]. The weight average molecular weight ($\bar{M}_w$) of PBO, PBZT and ABPBO are 14 000, 25 000 and 46 000, respectively, which were estimated by Mark–Houwink equations [22]. PBO–ABPBO samples were synthesized by random copolymerization, illustrated in Ref. [23], and they have an intrinsic viscosity of 6.7 dl g^{-1} in pure methanesulfonic acid (MSA) at 25°C. MSA was obtained from Sigma Chemical Co. For comparison with polymers above, PBO–PBOC2 sample was synthesized by condensation copolymerization of the tetrafunctional monomer 2,4-diamino-1,5-benzenediol (DABDO) dihydrochloride with aromatic and succinic acid in poly (phosphoric) acid (PPA). The PBO model compound: 2,6-diphenylbenzo[1,2-d:5,4-d′]bisoxazole (Model 1 for short), the PBO dimer and the PBO–ABPBO model compound (Model 2 for short) were also synthesized in our laboratory according to Refs. [8,24] and our unpublished reports. All these copolymers and compounds are illustrated in Fig. 2.

The polymers were employed as thin films, which were extracted on heated glass board and then immersed in a large volume of cold water for at least 3 days to remove solvent PPA completely; the water bath was checked with pH papers to assure that it was neutral. Then the films were dried in air. The PBZs samples were washed by acetone and deionized water and then dried sufficiently to minimize the absorbed moisture before performing characterization. PBO–PBOC2 film was heat-treated at 350°C for 15 min before performing EPR characterization.

$FeCl_3 \cdot 6H_2O$-doped PBZT samples were prepared by immersing the PBZT films in a concentrated $FeCl_3 \cdot 6H_2O$ solution in nitromethane in a sealed bottle. The doping process lasted 12 days in order to perform the doping reaction fully. After the doping, the golden PBZT film turned red. One sample was dried in air; another one, for comparison, was washed by deionized water in a beak for seven or more days until there was no $FeCl_3 \cdot 6H_2O$ dissolved in the water.

Wide-angle X-ray diffraction (WAXD) 2θ scans were collected in a range of 5–60° on a Rigaku D/max-rB rotating anode X-ray generator with CuKα ($\lambda = 0.15401$ nm) radiation operated at 100 mA and 40 kV.

EPR mesurements were performed on a BRUKER ER 200D-SRC Spectrometer operating at X-band using a 100 kHz magnetic field modulation. The PBZ films and the model compounds with approximately the same weight were set directly in EPR tubes. Quantitative EPR

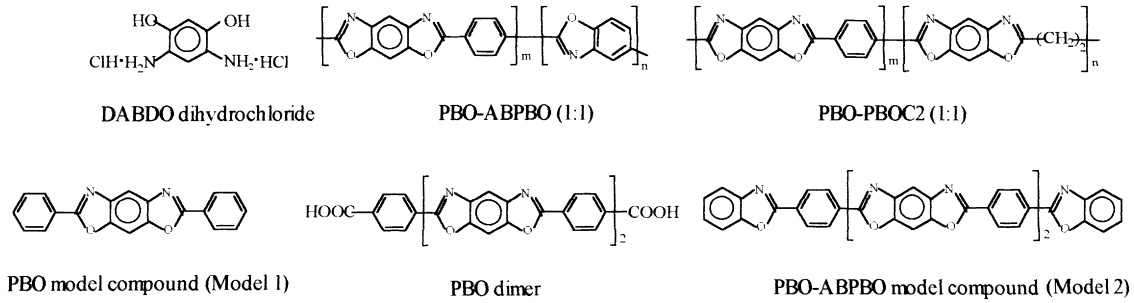

Fig. 2. Compounds and co-polymers for comparison.

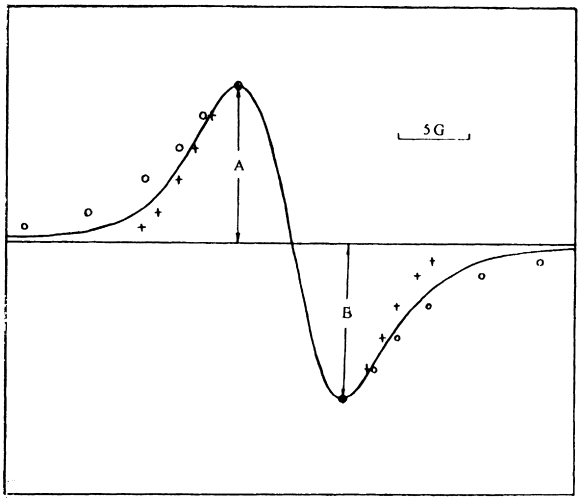

Fig. 3. Typical EPR spectrum of poly(benzazole)s and their model compounds considered here at room temperature. The cycles and crosses represent a Lorentzian derivative curve and a Gaussian curve having the same peak-to-peak amplitude and linewidth as the spectrum, respectively.

measurements were monitored by comparison to a diamond standard with about 3.4×10^{14} spins per gram.

Ion implantation was done at the Shanghai Institute of Metallurgy, using a ULVAC 1M-200M semiconductor ion implanter. The entire set of polymers was implanted under identical conditions: N^+ ions with energy of 170 keV, fluences of 1.0×10^{15}–3.0×10^{16} ions cm^{-2} and dose rates (or beam current) of 2 $\mu A\ cm^{-2}$.

Raman spectra of the implanted polymers were taken at the University of Leeds, UK, with a Renishaw Raman microscope with two possible exciting lasers available (a HeNe at 633 nm and an IP diode laser at 780 nm). The microscope has a computer-controlled stage that will allow the sample to be mapped in the *x*, *y* and *z* directions with spectral resolution $\sim 1\ cm^{-1}$ and resolution of ~ 1 mm, with a depth of field in the *z* direction of ~ 2 mm.

The samples were allowed to cool down to room temperature before measuring the conductivity with the standard four-point probe technique.

3. Results and discussion

3.1. EPR of poly(benzazole)s and other compounds considered herein

It is evident that the poly(benzazole)s and their model compounds represented here are paramagnetic and the spin concentrations are sufficiently high to suggest that the paramagnetic centers are intrinsic. This conclusion is also supported by the stability of the spin concentrations with various treating procedures. The intermediate shape between Gaussian and Lorentzian shown for PBO (Fig. 3) are typical for the polymers considered here, and spin concentrations are typically of the order of 10^{15} spins per gram, which corresponds to one unpaired spin per 2.3–4.4 × 10^6 repeat units (Table 1) (note that those values are only approximate due to the difficulty of analyzing). There is no EPR signal in DABDO dihydrochloride, one of the monomers for preparing PBO. The spin concentrations of the poly(benzazole)s are drastically less than those of poly(pyrrole) (PP) ($\sim 10^{19}$ spins per gram) [25], *trans*-polyacetylene (PA) ($\sim 10^{19}$ spins per gram) [26] and poly(*p*-phenylene) (PPP) ($\sim 10^{18}$ spins per gram) [27]. As-received PBO exhibits a spin concentration of 1.1×10^{15} spins per gram, while as-received PBZT displays a slightly smaller value of 8.6×10^{14} spins per gram, which is consistent with the previous studies on the spin concentration difference of the ladder polymers consisting of different heteroatoms [18].

The typical EPR signal of the poly(benzazole)s and their model compounds is a singlet without resolved hyperfine splitting, thus no direct information about the nature of the radical species can be obtained from the EPR spectrum, which is in agreement with the earlier studies [17,28]. This kind of EPR signal is similar to those of other conjugated polymers, for examples, PA [26], PPP [27] and poly(*p*-phenylene sulfide) (PPS) [29].

As to conjugated polymers with degenerate structures, such as *trans*-PA, the EPR spectra of the undoped and doped polymers can be rationalized in terms of the soliton defect model [30,31]. But this is not the case with the PPP [32] and the poly(benzazole)s.

Table 1
Spin concentrations (N_s) for samples considered here at room temperature

Samples	N_s ($\times 10^{15}$ spins per gram)	Conjugation units per spin ($\times 10^5$)
DABDO dihydrochloride	0	–
PBO model compound	0.2	–
PBO dimer	2.2	–
PBO–ABPBO model compound	3.5	–
PBO	1.1	23
PBZT	0.9	27
PBO–ABPBO	1.4	25[a]
PBO–PBOC2	1.1	–
ABPBO	1.2	44 (22[a])

[a] Equivalent number using one PBO repeat unit as one conjugation unit for comparison.

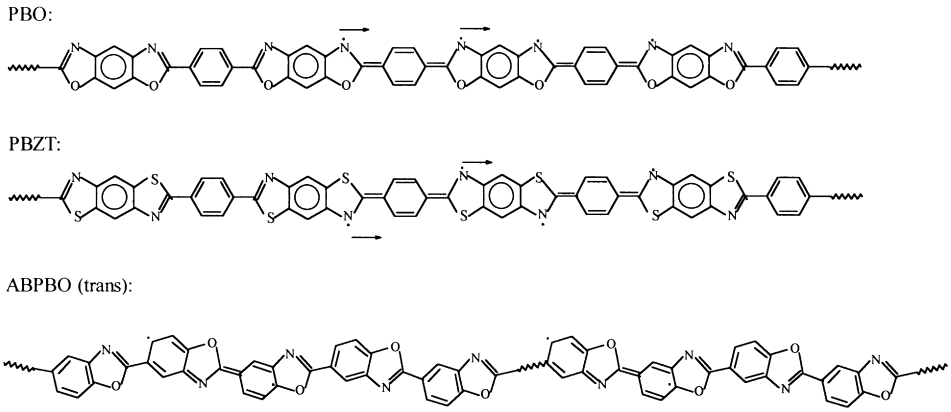

Fig. 4. Schematic representations of hypothetical soliton–antisoliton in PBO, PBZT and ABPBO.

As to conjugated polymers, such as the polymers studied in this paper, the two resonance structures of the phenyl ring or heteroring are not degenerate. That is to say, they are the systems with unique ground states. Contrary to *trans*-PA, the benzenoid and quinoid forms are not energetically equivalent, the quinoid structure being substantially higher in energy [33]. Nevertheless, the quinoid structure also exists in the polymer chain [34]. A neutral defect in this case corresponds to the boundary between benzenoid and quinoid structures. Because the two resonance structures are not degenerate, defects in the poly(benzazole)s must exist in pairs: soliton–antisoliton, as illustrated in Fig. 4.

From the values of the spin concentrations, it is evidently difficult for these neutral defects to be formed and extend over a long range of polymer backbone chain. The neutral defects on the poly(benzazole)s are confined and will recombine, but the combination of a neutral defect with a positively charged defect aroused in the polymerization will give a stable polaron [33].

The main results of the EPR study, including electron Zeeman *g*-factor, peak-to-peak line width ΔH_{pp} and asymmetry parameter defined by the ratio *A*/*B* of the peak heights *A* and *B* (Fig. 3) are summarized in Table 2.

The average *g*-values for the as-received poly(benzazole)s and their model compounds vary from 2.0034 to 2.0050, which is in agreement with the previous reports cited above [18,28] This is in marked contrast to a typical isotropic *g*-value of ~2.0023 observed for *trans*-PA and ~2.0025 for PPP, a *g*-value that is essentially equal to the free electron value. In conjugated polymers as illustrated above, the paramagnetic center, i.e. unpaired electron is not expected to be localized on one atom but rather is anticipated to exist in a delocalized molecular orbital (MO) as a linear combination of atomic orbital (LCAO). The observed *g*-shifts will depend on the spin–orbit coupling constants of the individual atomic orbitals and the extent to which each atomic orbital participates in the highest occupied molecular orbitals (HOMO) [18]. The difference between the *g*-values of the poly(benzazole)s and the free electron value could be rationalized as the participated nitrogen in the HOMO, since spin–orbit coupling with nitrogen would give rise to a large shift from the typical carbon-centered radical value of 2.0025 [28].

The linewidths of EPR spectra, ΔH_{pp}, for the poly(benzazole)s and their model compounds range from 6.0 to 10.0 G approximately. Compared with 1.46 G for *trans*-PA [35] and 0.67 G for poly(thiophene) [36], the ΔH_{pp} for heteroatom-centered conjugated polymers such as poly(benzazole)s and PPS [29] are rather large. The linewidth indicates the degree of delocalization of unpaired electrons by motion, and/or by exchange. The narrower is the linewidth, the greater is the delocalization on the conjugated polymer chain. Transport through nitrogen is predicted to be somewhat retarded relative to carbon, and oxygen or sulfur is not expected to participate in the π-conjugation [37]. Moreover, there is no general temperature-dependent line narrowing on warming from 100 K to room temperature, as shown in Fig. 5. Thus, a "confined" static defect on the poly(benzazole)s chain described above could also be supported by the broad temperature-independent EPR lines. By comparison of the linewidths of EPR spectra of poly (benzazole)s films, low-molecular weight model compounds and PBO–PBOC2 film, which have different

Table 2
EPR parameters of the samples considered here at room temperature

Parameter	PBO	PBZT	PBO–ABPBO	PBO–PBOC2	ABPBO	Model 1	PBO dimer	Model 2
g	2.0041	2.0045	2.0043	2.0045	2.0043	2.0034	2.0042	2.0045
ΔH_{pp}	8.0	8.7	9.8	7.2	7.6	7.3	7.1	9.2
A/*B*	1.28	1.31	1.23	1.49	1.14	0.96	0.95	0.95

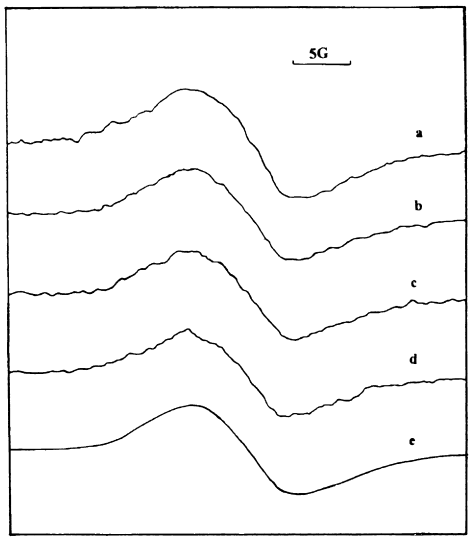

Fig. 5. EPR spectra of heat-treated PBZT (350°C, 10 min) measured at various temperatures: (a) 100 K; (b) 150 K; (c) 200 K; (d) 250 K; and (e) room temperature.

conjugation lengths, one can conclude that the conjugation length has a weak effect on the delocalization of the spin centers over the polymer chain. That is to say, the number of conjugation units over which the unpaired electron is delocalized is no more than 2.

Differences between the EPR signals involve especially the asymmetry of their lineshape. EPR spectra of conduction electrons in metals exhibit a Dysonian lineshape, provided the dimensions of the sample are large in comparison to the skin depth [38]. For the model compounds, the lines are almost symmetrical ($A/B = 0.95$) with intermediate shapes between Gaussian and Lorentizian. While the poly(benzazole) films show a slight asymmetry, the highest A/B ratio is 1.49 for the as-received ABPBO film. This ratio is reproducible and definitely not 1.0.

3.2. Effect of heat treatment on the EPR of poly(benzazole)s

Effect of heat treatment on the EPR parameters of the poly(benzazole)s is shown in Table 3. There is no significant change in the g-values for the poly(benzazole)s heat-treated at various temperatures, except for the cases of PBO and PBZT samples heat-treated at 550°C, 10 min. As to those cases, the g-factor changes from the typical value ~2.0045 to ~2.0035, which will be discussed in the Section 3.4. Heat treatment can reduce defects in the as-received poly(benzazole) films, make residual solvent PPA release from the films and promote the completion of the cyclization reaction, which are advantageous to the molecular regularity, the length of the conjugated system in the polymer chain and the packing of the chains [39].

With the increase of the conjugation length, the spin centers are expected to be delocalized over more conjugation units, which consequently will result in the decrease of the linewidth of the EPR spectra, i.e. “motion narrowing”. Yet this effect is not very significant, the linewidths decrease slightly for the PBO, PBZT and PBO–ABPBO samples with the increase of the heat-treatment temperature (Fig. 6). As to ABPBO samples, there is even a small increase. Such facts also corroborate the “confined” static defect model as suggested in the previous paragraph.

As discussed in our previous studies [40], there exists residual phosphoric acid partly in the form of associating with the amino group in the polymer molecule chain, as

Table 3
EPR parameters of as-received and heat-treated poly(benzazole)s at room temperature

Sample		g	ΔH_{pp} (G)	A/B	N_s (10^{14} spins per gram)
PBO	As-received	2.0041	8.0	1.28	11.4
	250°C, 10 min	2.0047	7.47	1.28	21.3
	350°C, 10 min	2.0047	7.73	1.17	8.7
	550°C, 10 min	2.0036	7.23	1.03	5.1
PBZT	As-received	2.0045	8.67	1.31	8.3
	250°C, 10 min	2.0050	8.53	1.19	7.1
	350°C, 10 min	2.0044	8.67	1.05	3.0
	550°C, 10 min	2.0031	6.13	0.93	6.6
PBO–ABPBO	As-received	2.0043	9.84	1.23	17.5
	150°C, 10 min	2.0043	9.65	1.05	13.7
	250°C, 10 min	2.0044	9.33	1.25	15.9
	350°C, 10 min	2.0043	8.80	1.03	7.7
	450°C, 10 min	2.0049	7.6	1.26	4.7
	550°C, 10 min	2.0044	7.6	0.97	4.0
ABPBO	As-received	2.0045	7.2	1.49	12.1
	250°C, 10 min	2.0046	7.68	1.36	11.7
	350°C, 10 min	2.0050	7.73	1.46	10.6
	450°C, 10 min	2.0047	8.53	1.28	8.2
	550°C, 10 min	2.0041	7.48	1.14	7.2

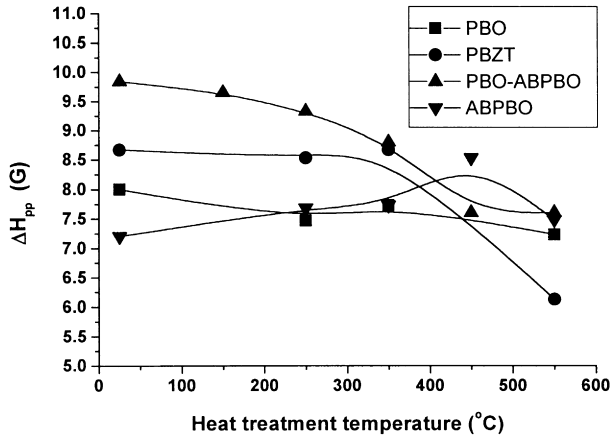

Fig. 6. Effect of heat-treatment temperature on the linewidths of the EPR spectra of the poly(benzazole)s at room temperature.

shown in Fig. 7. And element analysis on the phosphor content in the PBZT film after heat treatment at different temperatures also shows that the phosphor content in the as-received PBZT film is about 0.8 wt.% [41].

The phosphor content in poly(benzazole)s films plays a significant role in the EPR lineshape and the spin concentrations of the poly(benzazole)s before and after heat treatment. Illustrated in Fig. 8, EPR lines of the as-received PBZT sample and the PBZT sample heat-treated at 250°C for 10 min are different from those of the PBZT samples heat-treated at 350°C or more. There is a deviation from the pure normal shape around the center in the EPR lines of the as-received PBZT sample and the PBZT sample heat-treated at 250°C for 10 min. This fact can be explained as the result of electron spin density at ^{31}P. When PBZT forms an adduct with PPA, even a doublet structure appears in the EPR spectrum [18,28].

As the result of the small amount of phosphoric acid in the as-received poly(benzazole)s, positively charged defects will form stable polarons by combination with neutral defects. With the decrease of the phosphor content induced by heat treatment, the amount of positive-charged defect also reduces, which consequently results in that parts of the stable polarons are transformed to unstable soliton–antisoliton pairs. These neutral soliton–antisoliton defects are liable to approach each other, and finally diminish. This process is shown schematically in Fig. 9. Thus, the above discussion may explain the tendency of A/B and N_s to reduce with the heat-treatment temperature (see Table 3).

The trace of phosphoric acid in the as-received poly(benzazole)s causes the asymmetric EPR lines with A/B ratios of

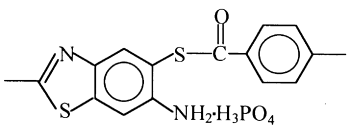

Fig. 7. Schematic structure of uncompleted cyclization segment of PBZT.

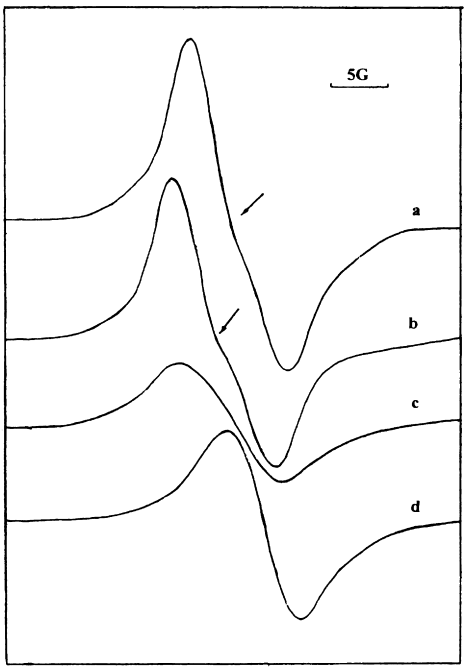

Fig. 8. EPR spectra of as-received (a) and heat-treated PBZT films at various temperatures (b, 250°C, 10 min; c, 350°C, 10 min; d, 550°C, 10 min), Gain (a–c), 8×10^4; (d) 4×10^4.

more than 1.0. This asymmetric lineshape reflects the change in the conductivity properties during heat treatment, while our earlier investigation [42] on the conductivity of the pristine PBZT films shows there is no significant correlation between the conductivity and the heat-treatment temperature. It may be rationalized as that the phosphoric acid content and the conjugation length, two factors may have an influence on the conductivity of the poly(benzazole)s, tend to change in the opposite directions by heat treatment. Moreover, these two factors are both quantitatively insignificant as indicated above.

3.3. EPR of $FeCl_3{\cdot}6H_2O$-doped PBZT

Here we present $FeCl_3{\cdot}6H_2O$-doped PBZT not for better conductivity properties of PBZT, but for corroborating the polaron, bipolaron model of the poly(benzazole)s. The EPR spectra of the as-received PBZT, washed $FeCl_3{\cdot}6H_2O$-doped PBZT and the as-received $FeCl_3{\cdot}6H_2O$-doped PBZT are shown in Fig. 10. The doping level of sample b is lower than that of sample c due to the washing-off of the dopant.

By comparing the intensity of the EPR spectra of the as-received PBZT and the $FeCl_3{\cdot}6H_2O$-doped PBZT samples, it can be seen that the spin concentration decreases from 8.3×10^{14} spins per gram (a) to 2.5×10^{14} spins per gram (b) without significant change of the position and linewidth of the EPR signal after the doping. Moreover, the spin concentration decreases further to 1.8×10^{14} spins per gram (c) with the increase of the doping level. The tendency of the spin concentration to decrease can be explained in

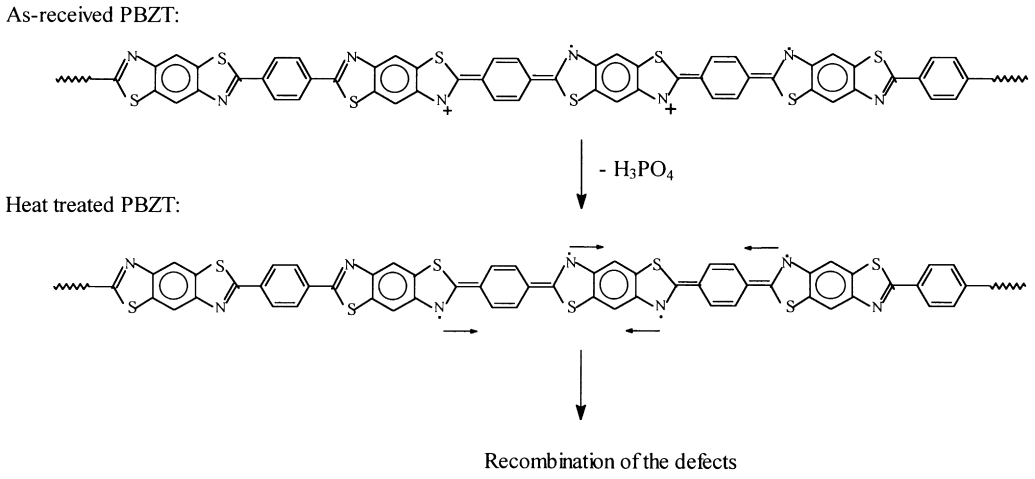

Fig. 9. Schematic process of heat-treatment on PBZT.

terms of bipolaron, which carries no spin [33]. The doping process leads more and more to double charging of the same chain segments after the formation of polaron induced by phosphoric acid in the as-received PBZT, as discussed in Section 3.2. Thus such spinless bipolaron are formed as illustrated in Fig. 11 and the EPR intensity falls. And there is no very broad signal with a *g*-value slightly greater than 2.0023 and a width of the order of 500 G for $[FeCl_4]^-$ doping species as illustrated in $FeCl_3$-doped PA [43,44].

It was mentioned above that the lineshape changed after the doping. Doping of PBZT films with $FeCl_3{\cdot}6H_2O$ gives an asymmetric and anisotropic EPR spectrum with $g_x \neq g_y \neq g_z$ ($g_x \neq 2.0100$, $g_y = 2.0073$, $g_z = 2.0003$ for sample b; $g_x = 2.0100$, $g_y = 2.0078$, $g_z = 2.0007$ for sample c). This induced anisotropy might result from the intercalation of the PBZT films with $FeCl_3{\cdot}6H_2O$, which can be seen from the comparison of the X-ray diffraction spectra (shown in Fig. 12) of the PBZT films before and after the doping. Previous to doping, the PBZT film exhibits two diffraction peaks located at $2\theta = 15.5°$ (peak A) and $2\theta = 25.8°$ (peak B), which correspond to the close packing of the PBZT molecules side-by-side at 0.588 nm in *a* direction and face-to-face at 0.354 nm in the *b* direction [45]; while after doping, the dopant intercalation [46,47] on alternate close-packed planes of polymer chains. Two new, long-spacing X-ray diffraction peaks at $2\theta = 22.8°$ (0.390 nm) and $2\theta = 35.5°$ (0.253 nm) arise for the PBZT/$FeCl_3{\cdot}6H_2O$ systems, which can be interpreted as the distance between two layers of dopant molecules or dopant-rich PBZT molecules separated by a loose-packed plane of PBZT chains.

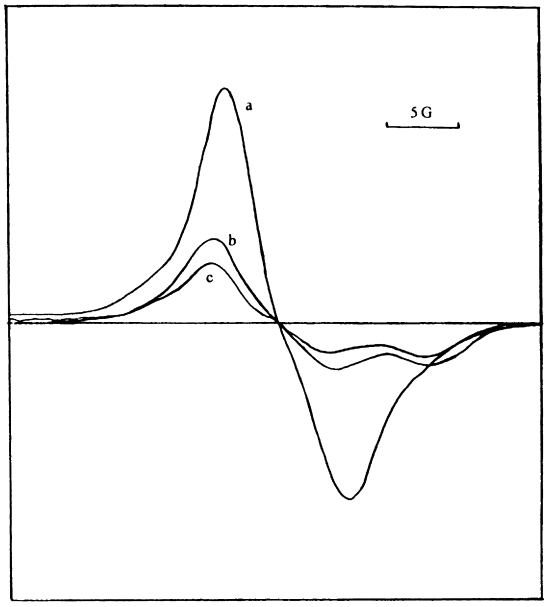

Fig. 10. EPR spectra of as-received PBZT (a), $FeCl_3{\cdot}6H_2O$-doped PBZT after washing (b) and as-received $FeCl_3{\cdot}6H_2O$-doped PBZT (c).

The asymmetry of the EPR lines increases with the doping of $FeCl_3{\cdot}6H_2O$. As depicted in Fig. 10, the *A*/*B* ratio changes from 1.19 (sample a) to 1.76 (sample b), then to 2.00 (sample c), which is consistent with metallic behavior at high doping levels.

The broad EPR spectra of $FeCl_3{\cdot}6H_2O$-doped PBZT indicate that the charge carriers, bipolarons are localized in the conjugation systems. This fact of conjugation with the EPR studies of the pristine poly(benzazole)s discussed in the paragraphs above may provide a useful explanation for the lower doping-induced conductivity of poly(benzazole)s compared with other conjugated polymers such as *trans*-PA.

3.4. N^+ implantation of poly(benzazole)s

Table 4 shows the measured room-temperature conductivity of the N^+-implanted PBZT and PBO films with various amount of N^+ implantation. It can be seen in Table 4 that the room-temperature conductivity of the implanted poly(benzazole)s increases with the amount of N^+ implantation. The results are significantly higher than that obtained by conventional doping technique [14], which is similar to the case of ^{84}Kr implantation of poly(benzazole)s of

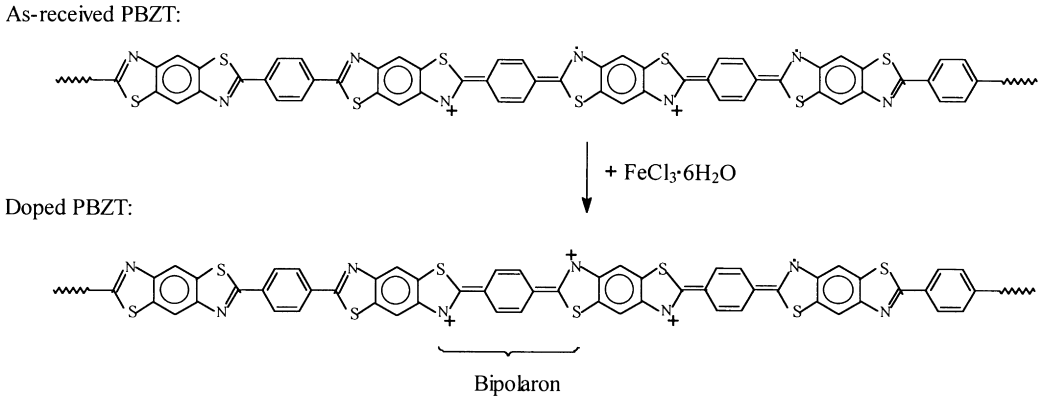

Fig. 11. Schematic process of $FeCl_3 \cdot 6H_2O$-doping PBZT and the formation of a bipolaron.

Refs. [15,16]. In their papers, the range of the ions in these polymers is small (<1 μm) compared to the thickness (25 μm or more) in the implantation under 200 keV energy, 2 μA cm^{-2} beam current and 4×10^{16} ion cm^{-2}. So, the depths of the N^+-implanted layer are even smaller under our present conditions, namely, 170 keV energy, 2 μA cm^{-2} beam current and 1×10^{15}–3×10^{16} ion cm^{-2}.

In order to elucidate the mechanism of the conductivity of N^+-implanted poly(benzazole)s, we perfomed EPR studies and Raman spectrual studies. EPR studies show different results in contrast to doping-induced conductivity mechanism. The singlet EPR signal for N^+-implanted poly(benzazole)s has a spin concentration comparable to those of the pristine poly(benzazole)s. Contrary to $FeCl_3 \cdot 6H_2O$-doped PBZT, there is no significant decrease as the dose of N^+ is increasing. And, the EPR lines of the N^+-implanted poly(benzazole)s are almost symmetric, which is completely different from those of the $FeCl_3 \cdot 6H_2O$-doped PBZT and the as-received poly(benzazole)s. Furthermore, the typical value of *g*-factor of N^+-implanted poly(benzazole)s with various doses of N^+ is 2.0030, which is less than the typical value, 2.0045 for the pristine poly(benzazole)s mentioned above. These later two phenomena of EPR spectra of N^+-implanted poly(benzazole)s are reminiscent of the EPR spectra of PBO and PBZT films heat-treated at 550°C in the previous paragraph. Ion implantation can also be considered as ion bombardment with high temperature, so it brings about the results similar to the heat treatment at elevated temperatures.

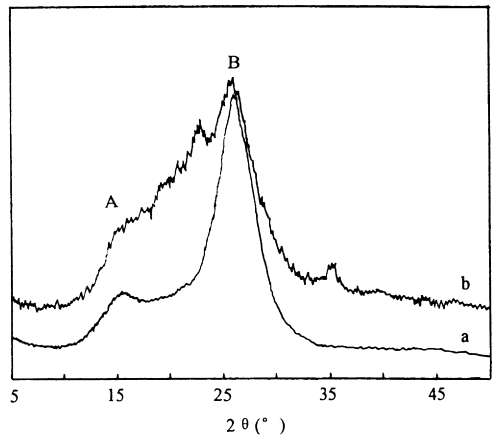

Fig. 12. Comparison of the X-ray diffraction spectra for as-received PBZT films before (a) and after (b) the doping with $FeCl_3 \cdot 6H_2O$.

The above phenomena indicate that there is a change in the structure of the poly(benzazole)s after N^+-implantation. The investigations of Jenekhe et al. [15] and Wang et al. [16] on ^{84}Kr-implanted poly(benzazole)s showed that there was significant reduction in the intensities of the heteroatoms (especially nitrogen sites) relative to the carbon peak in the comparison of the XPS spectra of both pristine and implanted PBO, which may be the cause of the *g*-shift from the typical value for nitrogen-centered unpaired electron. But how the polymer molecular structure changes and what kind of new structure arises after ion-implantation still need more detailed investigation, except the case of the surface of the ion-implanted poly(benzazole)s. Previous spectroscopic results and SEM pictures clearly supported the conclusion of substantial graphitization of implanted layers [15].

Raman spectrum of the N^+-implanted PBZT is shown in Fig. 13. There is a broad intense band in the 900–1760 cm^{-1} shift region, which is quite different from that of the ^{84}Kr-implanted PBZT with one intense band at 1480 cm^{-1} and a

Table 4
Conductivity of N^+-implanted PBZT and PBO films at room temperature

Sample	Amount of N^+ implantation (ions cm^{-2})	Conductivity (S cm^{-1})
PBZT	1×10^{15}	Undetectable
	5×10^{15}	Undetectable
	1×10^{16}	0.14
	3×10^{16}	0.22
PBO	1×10^{16}	2.58
	3×10^{16}	14.23

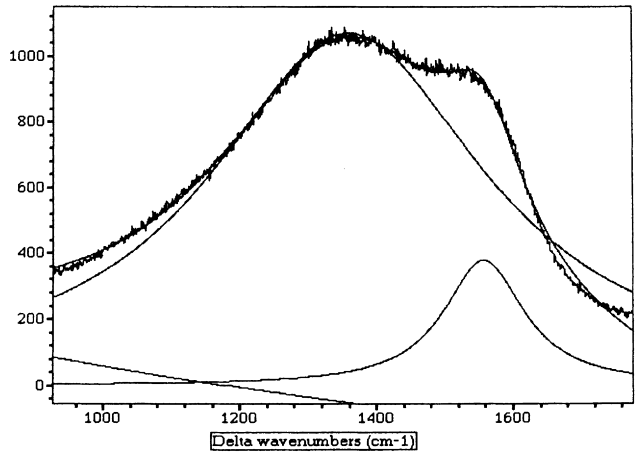

Fig. 13. Raman spectrum of N^+-implanted PBZT.

band of medium intensity at 1600 cm^{-1} [15]. However, our Raman spectrum also corroborates the result of graphitization of implanted layers. This broad intense band can be resolved into two separated bands as in Fig. 13, one band at 1359 cm^{-1} and the other at 1556 cm^{-1}, which correspond to the bands characteristic for the size factor of graphite and single-crystal graphite, respectively [48–51]. The ratio of the intensities of two bands at 1359 and 1556 cm^{-1} has an inverse relation with graphite particle size [51]. The color of PBO and PBZT films, N^+-implanted and heat-treated at 550°C, changes from golden to dark, while the color of PBO–ABPBO and ABPBO with higher molecular weights as indicated in Section 2 does not change as much. This aids to explain why the *g*-factors of PBO–ABPBO and ABPBO samples heat-treated at 550°C still show a nitrogen-centered character (see Table 3). The result indicates that the conductivity of N^+-implanted poly(benzazole)s is induced by the surface graphitization or carbonization of the ion-implantation, which indeed differs from the mechanism of the doping-induced conductivity.

4. Conclusion

EPR studies of the magnetic defect in the poly(benzazole)s and the model compounds are informative in explaining many experiment phenomena. Temperature dependence of the absorption spectra of poly(benzazole)s over the range 100–300 K is insignificant. And the heat-treatment temperature makes the EPR linewidth decrease slightly; as to ABPBO there is no pronounced correlation. $FeCl_3 \cdot 6H_2O$-doped PBZT was investigated for its EPR signals. The results of the analyses of the detailed lineshapes and linewidths were discussed in terms of the soliton–antisoliton, polaron and bipolaron model of the magnetic defect, which suggest a "confined" defect in the poly(benzazole)s chain. Such "confined" defects with low concentration can be thought as the cause of the lower doping-induced conductivity of poly(benzazole)s compared with other conjugated polymers such as *trans*-PA. The room-temperature conductivity of these implanted polymers, approximately 0.1–10 S cm^{-1}, is significantly higher than that of pristine polymers. EPR studies and Raman characterization of N^+-implanted PBZT and PBO aid to elucidate the conductivity mechanism. It was revealed through Raman spectrum that the conductivity was attributed partially to the graphite laminar formed in the process of ion-implantation, which was quite different from the mechanism of the doping-induced conducting polymers.

Acknowledgements

We gratefully acknowledge an illuminating discussion with Prof. Tao Chen and financial support granted by the National Natural Science Foundation of China. The number of financial item is 29774007.

References

[1] Skotheim TA, editor. Handbook of conducting polymers, vol. 2. New York: Marcel Dekker, 1986.
[2] Kuzmany H, Mehring M, Roth S, editors. Electronic properties of conjugated polymers Berlin: Springer, 1987.
[3] Kiess H, editor. Conjugated conducting polymers Berlin: Springer, 1992.
[4] Chien JCW. Polyacetylene: chemistry, physics and materials science. Orlando, FL: Academic Press, 1984 (and references therein).
[5] Etemad S, Heeger AJ, Macdiarmid AG. Ann Rev Phys Chem 1982;33:443–69.
[6] Heeger AJ. In: Skotheim TA, editor. Polyacetylene: new concepts and new phenomena, Handbook of conducting polymers, vol. 2. Marcel Dekker: New York, 1986. p. 729–56 (and references therein).
[7] Bernier P. In: Skotheim TA, editor. The magnetic properties of conjugated polymers: ESR studies of undoped and doped systems, Handbook of conducting polymers, vol. 2. Marcel Dekker: New York, 1986. p. 1099–125 (and references therein).
[8] Wolfe JF, Arnold FE. Macromolecules 1981;14(4):909–15.
[9] Wolfe JF, Loo BH, Arnold FE. Macromolecules 1981;14(4):915–20.
[10] Bhaumik D, Mark JE. J Polym Sci: Polym Phys Ed 1983;21(7): 1111–8.
[11] Nayak K, Mark JE. Makromol Chem 1985;186(10):2153–9.
[12] Bidarian A, Kadaba PK. J Mater Sci Lett 1988;7(9):922–3.
[13] Ulrich DR. Nonlinear optical and electroactive polymers: an review. In: Prasad PN, Ulrich DR, editors. Nonlinear optical and electroactive polymers, New York: Plenum Press, 1988. p. 1–11.
[14] Kim O-K. J Polym Sci: Polym Lett Ed 1982;20(12):663–6.
[15] Osaheni JA, Jenekhe SA, Burns A, Du G, Joo J, Wang Z, Epstein AJ, Wang C-S. Macromolecules 1992;25(21):5828–35.
[16] Wang C-S, Burkett J, Lee CY-C, Arnold FE. J Polym Sci: Part B Polym Phys 1993;31(12):1799–807.
[17] VanderHart DL, Wang EW, Eby RK, Fanconi BM, DeVries KL. Exploration of advanced characterization techniques for molecular composites. Report number: AFWAL-TR-85-4137, p. 78–82.
[18] Dalton LR, Thomson J, Nalwa HS. Polymer 1987;28(4):543–52.
[19] Wu P, Cao X, Huang H, Han Z. Mater Sci Prog 1989;3(2):188–92 (in Chinese).
[20] Wu P, Zhang X, Han Z. Funct Polym 1992;5(3):169–74 (in Chinese).
[21] Han Z, Lu Z, Shi X, Wu P. Acta Polym Sin 1997;2:141–6.
[22] Wolfe JF. Polybenzothiszoles and polybenzoxazoles. In: Mark HF, editor. Encyclopaedia of polymer science and engineering, 2nd ed. New York: Wiley, 1988. p. 601–35 (chap. 11).

[23] Wang S, Wu P, Han Z. In: Proceedings of National Polymer Conference of China, vol. 2, Shanghai, 1999. p. c75–6.
[24] Tsai TT, Arnold FE, Hwang WF. J Polym Sci: Part A Polym Chem 1989;27(9):2839–48.
[25] Scott JC, Pfluger P, Krounbi MT, Street GB. Phys Rev B 1983;28(4):2140–5.
[26] Goldberg IB, Crow HR, Newman PR, Heeger AJ, MacDiarmid AG. J Chem Phys 1979;70(3):1132–6.
[27] Jones MB, Kovacic P, Howe RF. J Polym Sci: Polym Chem Ed 1981;19(2):235–44.
[28] Young CL, Witney D, Vistnes AI, Dalton LR. Ann Rev Phys Chem 1986;37:459–91.
[29] Kispert LD, Files LA, Frommer JE, Shacklette LW, Chance RR. J Chem Phys 1983;78(8):4858–61.
[30] Su WP, Schieffer JR, Heeger AJ. Phys Rev Lett 1980;42(25):1698–701.
[31] Su WP, Schieffer JR, Heeger AJ. Phys Rev B 1980;22(4):2099–111.
[32] Kovacic P, Howe RF, Khoury I. J Polym Sci: Polym Chem Ed 1982;20(12):3305–12.
[33] Bredas JL, Chance RR, Silbey R. Phys Rev B 1982;26(10):5843–54.
[34] Whangbo M-H, Hoffmann R, Woodward RB. Proc R Soc London A 1979;366:23.
[35] Bernier P, Rolland M, Linaya C, Disi M. Polymer 1980;21(1):7–8.
[36] Tourillon G, Gourier D, Garnier P, Vivien D. J Phys Chem 1984;88(6):1049–51.
[37] Forner W, Seel M, Ladik J. J Chem Phys 1986;84(10):5910–8.
[38] Feher G, Kip AF. Phys Rev 1955;98:337.
[39] Wang S, Bao G, Lu Z, Wu P, Han Z. J Mater Sci 2000 (in press).
[40] Wu P, Yan M, Han Z, Lin X. Anal Chem 1989;17(2):1081–4 (in Chinese).
[41] Wu P, Yan M, Huang H, Han Z. Acta Polym Sin 1990;1:81–6.
[42] Wu P, Lu Z, Han Y, Han Z, Wang W, Lin F. Acta Polym Sin 1992;5:533–7.
[43] Pron A, Kulszewicz I, Billaud D, Przyluski J. JCS Chem Commun 1981;15:783–4.
[44] Pron A, Bernier P, Billaud D, Lefrant S. Solid State Commun 1983;46(8):587–90.
[45] Fratini AV, Lenhert PG, Resch TJ, Adams WW. Mater Res Soc Symp Proc 1989;134:431–45.
[46] Robin P, Pouget JP, Comes R, Gibson HW, Epstein AJ. Polymer 1983;24(12):1558–64.
[47] Baughman RH, Bredas JL, Chance RR, Elsenbaumer RL, Shacklette LW. Chem Rev 1982;82(2):209–22.
[48] Tuinstra F, Koenig JL. J Chem Phys 1970;53(3):1126–30.
[49] Elman BS, Dresselhaus MS, Dresselhaus G, Maby EW, Mazurek H. Phys Rev B 1981;24(2):1027–34.
[50] Elman BS, Shayegan M, Dresselhaus MS, Mazurek H, Dresselhaus G. Phys Rev B 1982;25(6):4142–55.
[51] Knight DS, White WB. J Mater Res 1989;4(2):385–93.